Intensity ratio of Lyman-α fine-structure components of Ti XXII in the JT-60 tokamak plasma

H. Kubo, A. Sakasai, Y. Koide, and T. Sugie
Naka Fusion Research Establishment, Japan Atomic Energy Research Institute, Naka-machi, Naka-gun, Ibaraki 311-02, Japan
(Received 29 July 1991; revised manuscript received 28 April 1992)

For the Lyman-α line of Ti XXII emitted from the JT-60 tokamak plasma, the intensity ratio of its fine-structure components ($1\,^2S_{1/2}$-$2\,^2P_{1/2,3/2}$) has been measured with a crystal spectrometer. Dependences of the ratio on plasma parameters have been investigated systematically in discharges with various heating modes. The ratio is found to vary by $\sim 10\%$. No satisfactory interpretation is given to the observed variation.

PACS number(s): 52.20.Hv, 52.25.Nr, 52.20.Fs

I. INTRODUCTION

Spectra of hydrogenlike heavy ions have been studied for the purpose of diagnosing hot plasmas [1]. The Lyman-α signal is strongest in the spectra. It is known theoretically that the intensity ratio of its fine-structure components ($1s\,^2S_{1/2}$-$2p\,^2P_{1/2,3/2}$) depends on the plasma density in the high-density region [2–4] (see Fig. 5 below). This is due to the collisional population mixing among the $2\,^2S_{1/2}$, $2\,^2P_{1/2}$, and $2\,^2P_{3/2}$ levels. The density of laser-produced plasmas was estimated from the observed and calculated intensity ratios [5]. In low-density plasmas, the intensity ratio is expected to be close to the ratio of the statistical weights of the upper levels ($=\frac{1}{2}$), although unresolved lines (magnetic dipole line $1s\,^2S_{1/2}$-$2s\,^2S_{1/2}$ and satellite lines) may give an additional contribution to the weaker component, leading to a slightly larger apparent ratio. However, there have been reports that the intensity ratio was appreciably larger than $\frac{1}{2}$ even in the low-density plasmas such as solar flares and tokamak plasmas. Phillips *et al.* reported that the intensity ratio for Mg XII was 0.64 in a solar flare with the density lower than 10^{18} m^{-3} [6]. Blanchet *et al.* also reported that the ratio for Ca XX was larger than $\frac{1}{2}$ in a solar flare [7]. The observed intensity ratio might be explained by non-negligible opacity [8,9]. Källne *et al.* reported that the ratio for S XVI in tokamak plasmas varied from 0.6 to 0.8 in the density range $(1-4)\times 10^{20}$ m^{-3} [10,11]. They found no apparent correlation between the ratio and n_e. On the other hand, Bombarda *et al.* reported that the intensity ratios for Ni XXVIII and Cr XXIV observed in the Joint European Torus (JET) tokamak plasma agreed within the experimental uncertainties with the theoretical values if the contribution from the magnetic dipole transition from the $2S_{1/2}$ state was taken into account [12,13]. Their observed ratios, however, were systematically larger than the prediction. Thus it is surprising that a phenomenon of the one-electron ions still remains unexplained.

In the following, we report a systematic measurement of the ratio, investigating its dependence on various plasma parameters.

II. EXPERIMENT

The spectrum of Ti XXII was recorded by a high-resolution ($\lambda/\Delta\lambda=7000$) curved crystal spectrometer [14] which viewed the center of the JT-60 tokamak [15] vertically. The spectrometer consisted of a (220) ($2d=3.84$ Å) silicon crystal and a microchannel plate detector (1024 channels) in the Johann configuration. The dimensions of the crystal and its radius of curvature were $60\times 30\times 1$ mm^3 and 2466 mm, respectively.

Figure 1 shows an example of the observed spectrum. The Lyman-α lines of Ti XXII and the satellite lines of Ti XXI were observed simultaneously. In this paper, the intensity ratio refers to the ratio of the signal integrated over the wavelength band of 2.4966±0.0026 Å ($1S_{1/2}$-$2P_{1/2}$) to the signal over the wavelength band of 2.4912±0.0027 Å ($1S_{1/2}$-$2P_{3/2}$). These wavelength bands are indicated with the horizontal lines in Fig. 1. The background level was determined from the signal observed simultaneously in the wavelength band of 2.4718–2.4806 Å. Figure 2 shows an example of time

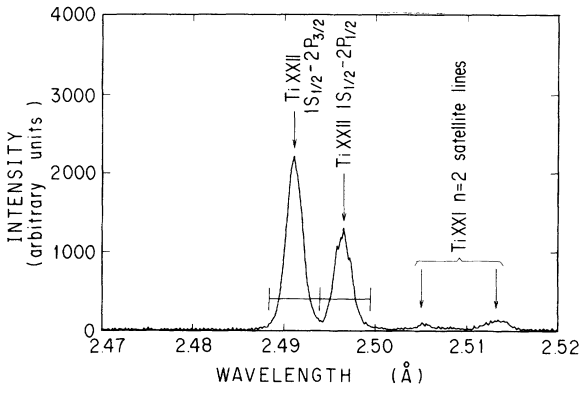

FIG. 1. Spectrum from H-like titanium. The spectrum was observed in a discharge with NB (21 MW) and LH rf (1.4 MW) heating. The signal was obtained by integrating the emission over 0.2 sec from the plasma with the central electron temperature 4 keV and the line average electron density 3.6×10^{19} m^{-3}.

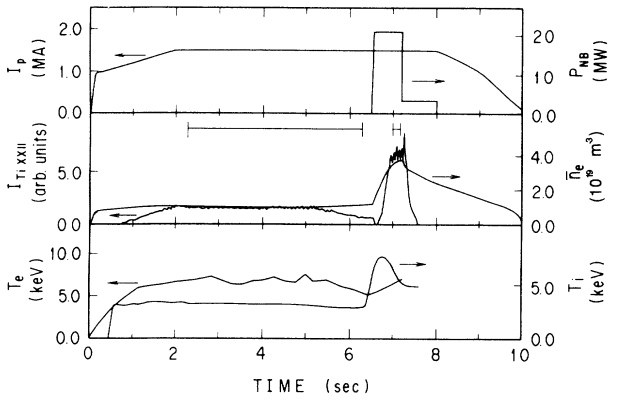

FIG. 2. Time evolutions of signals. I_P: plasma current; P_{NB}: NBI power; $I_{Ti\,XXII}$: intensity of TiXXII $1S_{1/2}$-$2P_{3/2}$; $\bar{n}_e$: line average electron density measured by a FIR interferometer; T_e: electron temperature measured by a soft-x-ray pulse-height analyzer (PHA); and T_i: ion temperature reduced from the Doppler broadening of Ti XXII $1S_{1/2}$-$2P_{3/2}$.

evolutions of the line intensity along with various quantities of the plasma. In this paper, we treat the line intensities from stationary plasmas obtained by integration of the emission intensities over the periods of 0.2–4 sec. For example, the two horizontal lines in the second column in Fig. 2 show the integration times for different heating conditions.

Figure 3 shows relations between the intensity ratio and various plasma parameters. The data were obtained in plasmas with a variety of plasma-heating modes:

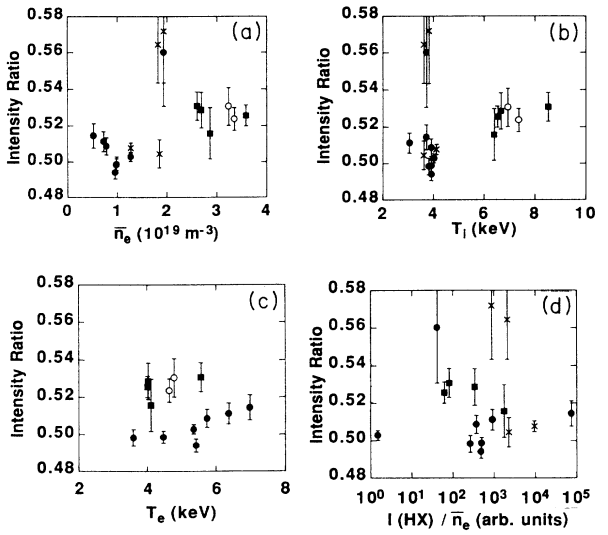

FIG. 3. Dependences of intensity ratio of Lyman-α fine-structure components of Ti XXII on plasma parameters: (a) electron density, (b) ion temperature, (c) electron temperature measured by Thomson scattering, and (d) $I(HX)/\bar{n}_e$, Here, $I(HX)$ refers to the intensity of hard x rays, with energy larger than 100 keV. The closed circles indicate data for Ohmically heated discharges, the open circles for NB-heated ones, the crosses for LH rf heated ones, and the squares for NB+LH rf heated ones.

Ohmic heating (OH), neutral-beam heating (NB, 22 MW), lower-hybrid electron heating (LH, 0.65–0.70 MW), and combined heating (NB 20–21 MW and LH 1.3–2.8 MW). The error bars indicate only the statistical errors in the observation. It was estimated from a ray-tracing calculation that the effects of the vignetting enhanced the intensity ratio by a factor of 1.11, apparently. The data shown in Fig. 3 have been corrected for the effect. The error due to the local variations of the detector sensitivity was estimated to be about 7%. The intensity ratio varies by ~10% from 0.494 to 0.572 in these plasmas. Figure 3(a) appears to indicate that the ratio increases with the electron density except for a few plasmas. Figure 3(b) also suggests that the ratio increases with the ion temperature. However, it should be noted that there is a correlation between the electron density and the ion temperature in our plasmas. This is because the plasmas with the high ion temperature were heated by the NB and the electron densities were also high in such plasmas. No correlation is detected between the intensity ratio and the electron temperature, as shown in Fig. 3(c). The abscissa of Fig. 3(d) is the hard-x-ray intensity divided by the electron density $[I(HX)/\bar{n}_e]$, and is a measure of the relative density of the suprathermal electrons. No correlation is found in this figure.

III. DISCUSSION

Figure 4 shows the transition processes in the energy-level diagram of Ti XXII. The energies of excited levels

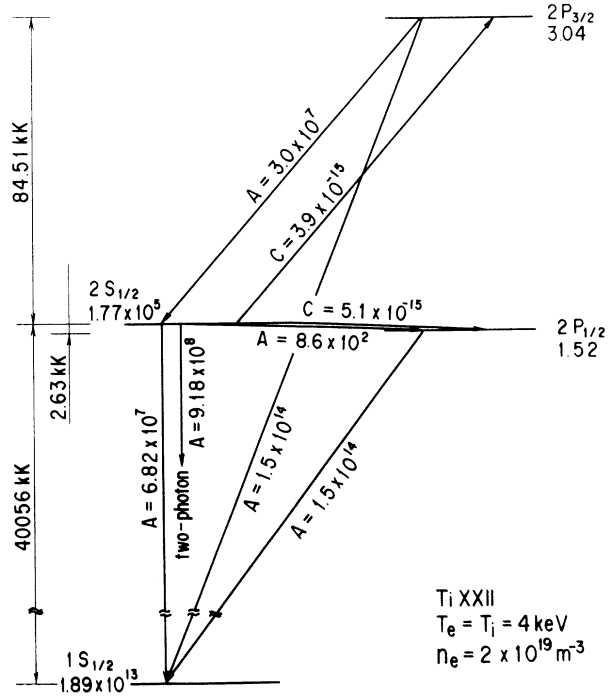

FIG. 4. Transition processes in the energy diagram of Ti XXII for the plasma with $T_e = T_i = 4$ keV, $n_e = 2 \times 10^{19}$ m^{-3}, and $Z_{eff} = 1$. The populations shown below the levels were obtained from the scaling of the result for Ca XX, which was calculated by the collisional radiative program [21].

were taken from Ref. [16]. A is the radiative transition probability (sec^{-1}). The probabilities for the magnetic dipole transition and the two photon transition from $2S_{1/2}$ were taken from Ref. [17]. Other transition probabilities were obtained from the scaling of the probabilities for H I [18,19]. C is the rate coefficient for excitation (deexcitation) induced by proton collisions [20] in units of m^3/sec. The populations calculated by the collisional radiative program (see below) are shown below each level in the figure. Because the energy difference between $2S_{1/2}$ and $2P_{1/2}$ is small, the spectral lines of $1S_{1/2}$-$2P_{1/2}$ and $1S_{1/2}$-$2S_{1/2}$ (magnetic dipole) are unresolved experimentally. Therefore the apparent intensity ratio tends to be larger than $\frac{1}{2}$. The contribution from the magnetic dipole line to the intensity ratio is 3% in the low-density region.

First, we discuss the dependence of the intensity ratio on the density. Figure 5 shows the intensity ratio calculated by the collisional radiative model which includes ion collisions [21]. In the high-density region [$n_p > \frac{1}{10}(A_{1S_{1/2}-2S_{1/2}}/C_{2S_{1/2}-2P_{1/2}})$, n_p is the plasma ion density], the relative intensity of $1S_{1/2}$-$2P_{1/2}$ increases owing to the population transfer by ion collisions from the metastable state $2S_{1/2}$ to $2P_{1/2}$. As clearly seen in Fig. 5, the densities of the JT-60 tokamak plasma are two orders of magnitude lower than the density at which the enhancement of the ratio takes place. This conclusion is unaffected even if we take into account the contribution from impurity ion collisions.

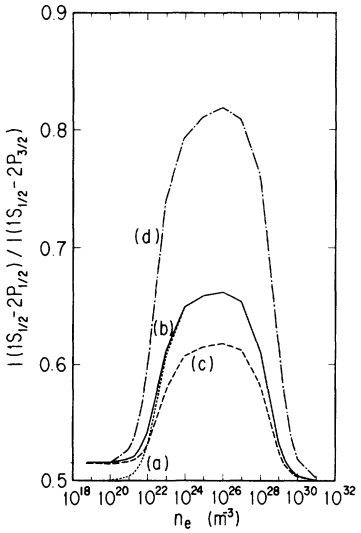

FIG. 5. Plots showing the intensity ratio of the Lyman-α doublets of Ti XXII as a function of the electron density. The intensity ratio was obtained from the scaling of the result for Ca XX, which was calculated by the collisional radiative program [21]. (a) Contribution from the magnetic dipole transition from the $2S_{1/2}$ state was not taken into account. The plasma is composed of ionized hydrogen with $T_e = T_i = 4$ keV. (b) Contribution from the magnetic dipole transition was taken into account. The plasma is composed of ionized hydrogen with $T_e = T_i = 4$ keV. (c) Contribution from the magnetic dipole transition was taken into account. The plasma is composed of ionized hydrogen with $T_e = T_i = 10$ keV. (d) Contribution from the magnetic dipole transition was taken into account. The plasma is composed of fully ionized oxygen with $T_e = T_i = 4$ keV.

Dielectronic satellite lines close to the Lyman-α lines may affect the apparent intensity ratio. The intensities (I_d) of these satellite lines relative to the resonance line are expressed as [22]

$$I_d = \frac{2.619\times10^{-4}}{T_e^{3/2}C_R(T_e)}\exp\left[\frac{-E_s^{(n)}}{T_e}\right]F_2(s)\ ,$$

where T_e is the electron temperature in keV, and C_R is the excitation rate for the total Ti XXII resonance transition $1s$-$2p$, and $E_s^{(n)}$ is the average energy of the autoionizing heliumlike states of a given n shell relative to the hydrogenlike ground state. The line factors $F_2(s)$ for satellite lines with $n = 2-5$ were tabulated in Ref. [22], and those for satellite lines with $n \geq 6$ are obtained by extrapolation with use of the appropriate scaling laws [23]. As a result, it is calculated that the contribution of unresolved satellite lines to the apparent intensity ratio is 1.5% at $T_e = 3.5$ keV, and the contribution decreases as the electron temperature increases.

As is suggested from the abscissa of Fig. 3(d), hard-x-ray radiation was observed in some discharges. This indicates the existence of suprathermal electrons whose velocity distribution is anisiotropic. The anisotropic electron collisions may produce alignment of the excited states; then the observed emission intensity may depend on the direction of the observation and the polarization response of the spectrometer [24]. Figure 6 shows the excitation and radiation scheme in the Kastler diagram. Because the duration of the electron collision is much shorter than the spin-orbit interaction time, the density matrix ρ of the $2P$ state can be diagonalized in the uncoupled basis ($lm_l sm_s$). The component of the density matrix in the coupled basis ($lsjm$) is expressed as [25]

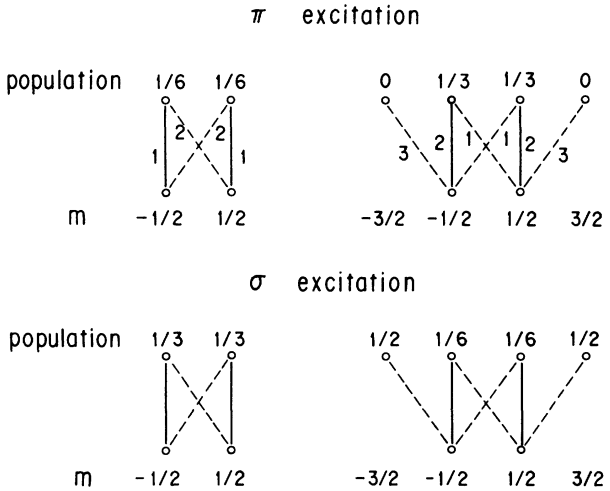

FIG. 6. Kastler diagram of $1S$-$2P$ transition.

$$\rho_{lsjm} = \sum_{m_l, m_s} (-1)^{2l-2s+2m}(2j+1) \times \begin{pmatrix} l & s & j \\ m_j & m_s & -m \end{pmatrix}^2 \rho_{lm_l sm_s} ,$$

where ( ) is the 3-j symbol. We consider two kinds of excitations in which $\Delta m_l = 0$ and $\Delta m_l = \pm 1$. We call the former case the π excitation and the latter the σ excitation. We then consider a spontaneous transition from (jm) to $(j'm')$. The emission radiation accompanying the transition with $\Delta m = 0$ is linearly polarized along the quantization axis (π component), and the light emitted in the transition with $\Delta m = \pm 1$ is circularly polarized in the plane perpendicular to the quantization axis (σ component). Each transition probability is proportional to

$$\begin{pmatrix} j & 1 & j' \\ -m & q & m' \end{pmatrix}^2 ,$$

where $q = 0$ and $q = \pm 1$ correspond to the π component and the σ component, respectively [25]. The relative line intensities of the π and σ components following the π and σ excitations are shown in Table I. In general, the intensity ratio differs from $\frac{1}{2}$. A crystal with its Bragg angle of 45° reflects only the light polarized perpendicularly to the incidence plane [26]. The Bragg angle of the present spectrometer was 40.6°, which was close to 45°. Therefore we assume that the polarization dependence of the reflection efficiency of the crystal is not much different from the ideal case. We take the quantization axis along the torodial direction (the direction of the momentum of the suprathermal electrons); then the incidence plane to the crystal was perpendicular to the quantization axis. Therefore the present measurement is close to the case of observing the π component with $\theta = \pi/2$ in Table I. The ratio of the excitation cross sections, $\sigma_{1s_0-2p_0}/(\sigma_{1s_0-2p_0}+2\sigma_{1s_0-2p_1})$, of Ti^{21+} for collisions with 100-keV electrons was calculated to be 0.300 in the nonrelativistic Coulomb-Born approximation [27]. It is known that the relativistic effect is small on the alignment [28], and we neglect this effect. The intensity ratio is estimated to be 0.53 even if all the electrons were anisotropic fast electrons with their energy of 100 keV. Thus the polarization effect cannot explain the observed result. In fact, the observed result [Fig. 3(d)] shows no dependence of the intensity ratio on the relative density on suprathermal electrons.

The radiative transition probability for $1S_{1/2}$-$2S_{1/2}$ is much smaller than that for $1S_{1/2}$-$2P_{1/2}$, resulting in a large population in $2S_{1/2}$ (Fig. 4). Therefore, if even a small amount of the wave function of $2P_{1/2}$ mixes into that of $2S_{1/2}$, the radiative transition probability $1S_{1/2}$-$2S_{1/2}$ increases appreciably and the signal observed in the wavelength band of the $1S_{1/2}$-$2P_{1/2}$ line increases. The variation of the apparent intensity ratio should appear approximately with the electronic field of 7×10^6 V/cm; The mixing rate is approximately $\frac{1}{10}(A_{1S_{1/2}-2S_{1/2}}/A_{1S_{1/2}-2P_{1/2}})^{1/2}$ (=0.8%). In the JT-60 tokamak plasma with $B_T = 4.5$ T and the ion temperature $T_i = 4$ keV, the electric field induced by the motional Stark effect is 6×10^3 V/cm. Therefore this Stark mixing effect cannot account for the experimental result.

TABLE I. Relative line intensities of the π and σ components. Here θ is the angle between the observation direction and the quantization axis.

	Observation			
	$\theta=0$	$\theta=\pi/2$		
Excitation		π Comp.	σ Comp.	Total
π excitation	(2,2)	(1,4)	(1,1)	(2,5)
σ excitation	(4,10)	(2,2)	(2,5)	(4,7)

When a spectral line is optically thick, the apparent intensity is affected. However, there is not such self-absorption for Lyman-α lines. As shown in Fig. 4, the population of $2S_{1/2}$ is much larger than that of $2P_{1/2}$, and population inversion occurs for these states. Under certain conditions, super-radiance, or amplification of spontaneous emission, could develop, leading to higher population in the lower level [29]. However, the population difference between the $2P_{1/2}$ and $2S_{1/2}$ states is smaller than the threshold by many orders. The fast ion induced by NB heating cannot affect the intensity ratio. Most (91%) of the observed plasma regions for the two lines were overlapped. Therefore the change of the observed plasma region caused by the Shafranov shift of the magnetic axis cannot affect the intensity ratio in the present measurement.

In this section, we have discussed possible causes of the variation of the intensity ratio. No existing model succeeds in interpreting the experiment.

ACKNOWLEDGMENTS

The authors would like to thank Professor T. Fujimoto of Kyoto University, Professor T. Kato of National Institute for Fusion Science, and Dr. H. Takeuchi of Japan Atomic Energy Research Institute for their helpful discussions. We thank Dr. R. W. P. McWhirter *et al.* for providing their program. We also thank Prof. R. Srivastava for providing his calculated results, and we wish to thank the staff of the JT-60 tokamak. We also wish to express our gratitude to Dr. A. Funahashi and Dr. Y. Shimomura.

[1] E. Källne and J. Källne, Phys. Scr. **T17**, 152 (1987).
[2] N. N. Ljepojevic, R. J. Hutcheon, and R. W. P. McWhirter, J. Phys. B **17**, 3057 (1984).
[3] G. J. Tallents, J. Phys. B **17**, 3677 (1984).
[4] N. N. Ljepojevic, R. W. P. McWhirter, and S. Volonté, J. Phys. B **15**, 3285 (1985).
[5] V. A. Boiko *et al.*, Fiz. Plazmy **4**, 97 (1978) [Sov. J. Plasma Phys. **4**, 54 (1978)].

[6] K. J. H. Phillips *et al.*, Astrophys. J. **256**, 774 (1982).
[7] L. Blanchet *et al.* Astron. Astrophys. **152**, 417 (1985).
[8] B. Sylwester *et al.*, Sol. Phys. **103**, 67 (1986).
[9] R. W. P. McWhirter and P. J. MacNeice, Sol. Phys. **107**, 323 (1987).
[10] E. Källne and J. Källne, Phys. Rev. Lett. **49**, 330 (1982).
[11] E. Källne and J. Källne, in *X-Ray and Atomic Inner-Shell Physics (University of Oregon, Eugene, Oregon),* Proceedings of the International Conference on X-Ray and Atomic Inner-Shell Physics, AIP Conf. Proc. No. 94, edited by B. Crasemann (AIP, New York, 1982), p. 463.
[12] F. Bombarda *et al.*, Phys. Rev. A **37**, 504 (1988).
[13] R. Bartiromo, F. Bombarda, and R. Giannella, Phys. Rev. A **40**, 7387 (1989).
[14] A. Sakasai *et al.*, Kaku Yugo Kenkyu **59**, 169 (1988) (special supplement).
[15] JT-60 Team (T. Abe *et al.*), in *Proceedings of the Eleventh International Conference on Plasma Physics and Controlled Nuclear Fusion Research, Kyoto, Japan, 1986* (International Atomic Energy Agency, Vienna, 1987), paper CN-47/A-I-1.
[16] G. W. Erickson, J. Phys. Chem. Ref. Data **6**, 831 (1977).
[17] F. A. Parpia and W. R. Johnson, Phys. Rev. A **26**, 1142 (1982).
[18] E. U. Condon and G. H. Shortley, *The Theory of Atomic Spectra* (Cambridge University Press, Cambridge, 1935).
[19] H. A. Bethe and E. E. Salpeter, *Quantum Mechanics of One- and Two-Electron Atoms* (Plenum, New York, 1977).
[20] V. P. Shevelko, I. Y. Skobelev, and A. V. Vinogradov, Phys. Scr. **16**, 123 (1977).
[21] N. N. Ljepojevic, R. J. Hutcheon, and J. Payne, Comput. Phys. Commun. **44**, 157 (1987).
[22] M. Bitter *et al.*, Phys. Rev. A **29**, 661 (1984).
[23] F. Bely-Dubau, A. H. Gabriel, and S. Volonte, Mon. Not. R. Astron. Soc. **189**, 801 (1979).
[24] U. Fano and J. H. Macek, Rev. Mod. Phys. **45**, 553 (1973).
[25] R. D. Cowan, *The Theory of Atomic Structure and Spectra* (University of California Press, Berkley, 1981).
[26] A. Bruck, Space Sci. Instrum. **2**, 53 (1976).
[27] R. Srivastava (private communication).
[28] M. Inokuchi, Rev. Mod. Phys. **43**, 297 (1971).
[29] J. C. MacGillvray and M. S. Feld, Phys. Rev. A **14**, 1169 (1976).